ACS APPLIED MATERIALS & INTERFACES

www.acsami.org

Research Article

Transient Elastomers with High Dielectric Permittivity for Actuators, Sensors, and Beyond

Yauhen Sheima, Johannes von Szczepanski, Patrick M. Danner, Tina Künniger, Arndt Remhof, Holger Frauenrath, and Dorina M. Opris*

Cite This: *ACS Appl. Mater. Interfaces* 2022, 14, 40257−40265

Read Online

ACCESS | Metrics & More | Article Recommendations | Supporting Information

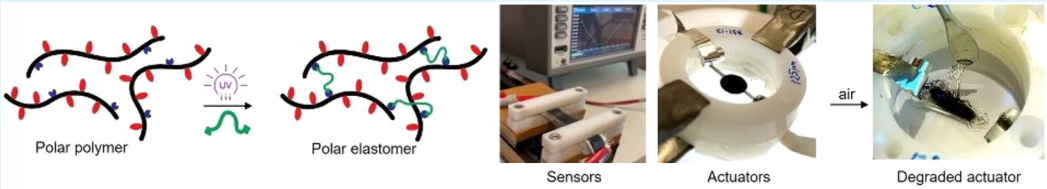

ABSTRACT: Dielectric elastomers (DEs) are key materials in actuators, sensors, energy harvesters, and stretchable electronics. These devices find applications in important emerging fields such as personalized medicine, renewable energy, and soft robotics. However, even after years of research, it is still a great challenge to achieve DEs with increased dielectric permittivity and fast recovery of initial shape when subjected to mechanical and electrical stress. Additionally, high dielectric permittivity elastomers that show reliable performance but disintegrate under normal environmental conditions are not known. Here, we show that polysiloxanes modified with amide groups give elastomers with a dielectric permittivity of 21, which is 7 times higher than regular silicone rubber, a strain at break that can reach 150%, and a mechanical loss factor tan δ below 0.05 at low frequencies. Actuators constructed from these elastomers respond to a low electric field of 6.2 V μm^{-1}, giving reliable lateral actuation of 4% for more than 30 000 cycles at 5 Hz. One survived 450 000 cycles at 10 Hz and 3.6 V μm^{-1}. The best actuator shows 10% lateral strain at 7.5 V μm^{-1}. Capacitive sensors offer a more than a 6-fold increase in sensitivity compared to standard silicone elastomers. The disintegrated material can be re-cross-linked when heated to elevated temperatures. In the future, our material could be used as dielectric in transient actuators, sensors, security devices, and disposable electronic patches for health monitoring.

KEYWORDS: *transient dielectrics, high dielectric permittivity elastomers, dielectric constant, transient actuators, transient sensors, low-voltage actuation, transient electronics*

1. INTRODUCTION

The annual global amount of electronic waste reached 50 million tons in 2017, which has a tremendous impact on the environment.[1,2] This impact could be significantly reduced with transient electronic devices that fully or partially disintegrate in nature.[3] To this end, transient functional materials are needed for substrates, conductors, semiconductors, and insulators.[4,5] Technologically relevant examples for device substrates are abundant and include water-soluble or biodegradable polymers such as polyvinylpyrrolidone (PVP), poly(lactic acid) (PLA), poly(vinyl alcohol) (PVA), poly(lactic-*co*-glycolic acid) (PLGA), chitosan, poly(lactic-*co*-glycolic) acid, polycaprolactone, cellulose, and silk.[4,6,7] By contrast, only a few examples of transient conductive and semiconductive polymer materials have been reported.[6,7] In particular, transient polymers for dielectrics are limited to PVA,[8] which lacks extensibility and has a low permittivity (ε' = 3).[9] To the best of our knowledge, no high dielectric permittivity elastomers are available that maintain their full properties and functionalities and show reliable performance but disintegrate when exposed to the ambient environment.[10] Such materials could be used as dielectric materials in transient stretchable electronics, dielectric elastomer actuators, stretchable capacitive sensors, security devices, degradable medical implants, and disposable electronic patches for health monitoring.[11]

Chemical modification of polymers with polar side groups is a promising approach for achieving high dielectric permittivity elastomers.[10,12−21] Despite decades of research in this field, few examples of high-permittivity elastomers show promising actuator performance.[22−29] Additionally, there is no report on high dielectric permittivity transient elastomers, which are chemical or physical networks of low-glass transition polar polymers that maintain their characteristics over a predeter-

Received: March 31, 2022
Accepted: August 11, 2022
Published: August 23, 2022

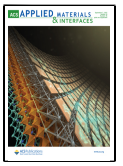

Scheme 1. Synthesis of Dimethylamide Modified Polysiloxane P Containing Polar Side Groups and Its Cross-Linking into Elastomeric Films E*x*

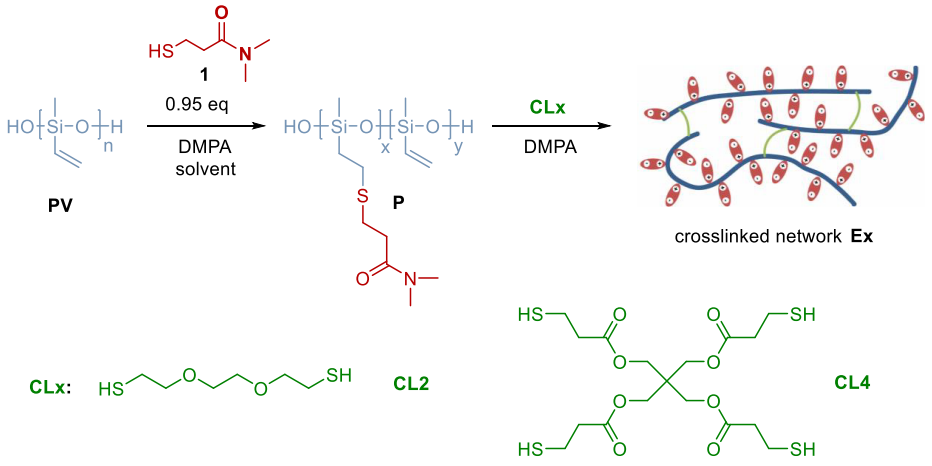

Table 1. Amount of Reagents Used to Synthesize Different Materials, the Elastic Modulus at 10% Strain ($Y_{10\%}$), Average Strain at Break (s_{av}), Storage Modulus (E'), and tan δ at 0.05 Hz

sample name	CL2[a] [μL]	CL4[a] [μL]	-SH in CL*x* [mmol]	-SH/Vinyl mol ratio[b]	$M_{x,eff}$[c]	$Y_{10\%}$ [kPa]	s_{av} [%]	E' @0.05 Hz [kPa]	tan δ @ 0.05 Hz	T_g [°C]
E1	20		0.049	0.32		111 ± 11	81 ± 31			
E2	40		0.098	0.64		297 ± 9	45 ± 12			
E3	55		0.135	0.88	28400	428 ± 6	39 ± 3	304 ± 47	0.0049 ± 0.0038	−41
E4	70		0.172	1.12		454 ± 13	32 ± 6			
E5	85		0.209	1.37		322 ± 24	37 ± 4			
E6	100		0.246	1.61		317 ± 36	60 ± 20			
E7	120		0.295	1.93		204 ± 7	60 ± 11			
E8	150		0.369	2.41		164 ± 11	80 ± 9			
E9	200		0.492	3.22	51700	112 ± 6	153 ± 26	167 ± 1	0.0066 ± 0.0042	−41
E10		64	0.135	0.88	15800	632 ± 53	28 ± 3	532 ± 38	0.0022 ± 0.00057	−37
E11		103	0.492	3.22	31500	363 ± 16	35 ± 4	267 ± 18	0.0055 ± 0.0021	−37

[a]Volume of **CL2** or **CL4** added (20 vol % solutions in THF) to **E*x*** (1 g). Stress−strain curves for different materials can be found in Figure S2. [b]Molar ratio of thiol in **CL*x*** to the vinyl group in **P**. [c]Densities of **E3** and **E9** were 1.1615, and those of **E10** and **E11** were 1.1325.

mined period but fully or partially disintegrate when exposed to stimuli.

Here, we report a class of dielectric elastomers with dielectric permittivities up to seven times higher than typical polydimethylsiloxanes, which slowly disintegrate when stored in ambient conditions. To this end, we functionalized polymethylvinylsiloxane (**PV**) with *N*,*N*-dimethyl-3-mercaptopropanamide and cross-linked the functionalized polysiloxanes via thiol−ene reaction with either 2,2′-(ethylenedioxy)-diethanethiol or pentaerythritol tetrakis(3-mercaptopropionate). The mechanical properties of the resulting materials could be tuned by the type and degree of cross-linking. Their dielectric permittivity showed a significant increase compared to unfunctionalized polyvinylsiloxane due to the high concentration of polar amide side groups, while their conductivity was still in the insulator range. Actuators and sensors constructed with these materials showed reliable and reversible responses at rather low electric fields. All properties were preserved in a dry environment. However, these dielectric materials slowly disintegrated under a normal environment, likely due to water uptake, which promotes depolymerization of the polysiloxane backbone catalyzed by the amide group.[30] The disintegrated material could be cross-linked again to an elastic network after being heated to elevated temperature, which may open the possibility of recycling.

2. RESULTS AND DISCUSSION

2.1. Synthesis. The two-step synthesis process toward cross-linked polar elastomers is presented in Scheme 1. First, **PV** (M_n = 105 480 g/mol, M_w = 375 000 g/mol, PDI = 3.55, Figure S1a) was functionalized with less than an equimolar amount of polar thiol (relative to the amount of vinyl groups in **PV**), using a UV-induced thiol−ene reaction to give polar prepolymer **P** (M_n = 71 700 g/mol, M_w = 139 600 g/mol, PDI = 1.95, Figure S1a) that remained stable over the course of at least 1 month when stored in a closed environment. The vinyl groups left unreacted in this step (approximately 3.3 mol % by ^{1}H NMR integration, Figure S1b) were subsequently used for cross-linking using a UV-induced thiol−ene reaction in the presence of 2,2-dimethoxy-2-phenyl acetophenone (DMPA) and two different thiols (**CL*x***), 2,2′-(ethylenedioxy)-diethanethiol (**CL2**), and pentaerythritol tetrakis(3-mercaptopropionate) (**CL4**). Thin films were cast by doctor-blading on either a poly(vinyl alcohol) sacrificial layer or Teflon. The films cross-linked within 5 min of UV light exposure. The properties of the elastomers were optimized by the amount of cross-linker used to give 11 different elastomers denoted as **E*x*** (x = 1−11). The reagents used to synthesize elastomers **E*x***

https://doi.org/10.1021/acsami.2c05631
ACS Appl. Mater. Interfaces 2022, 14, 40257−40265

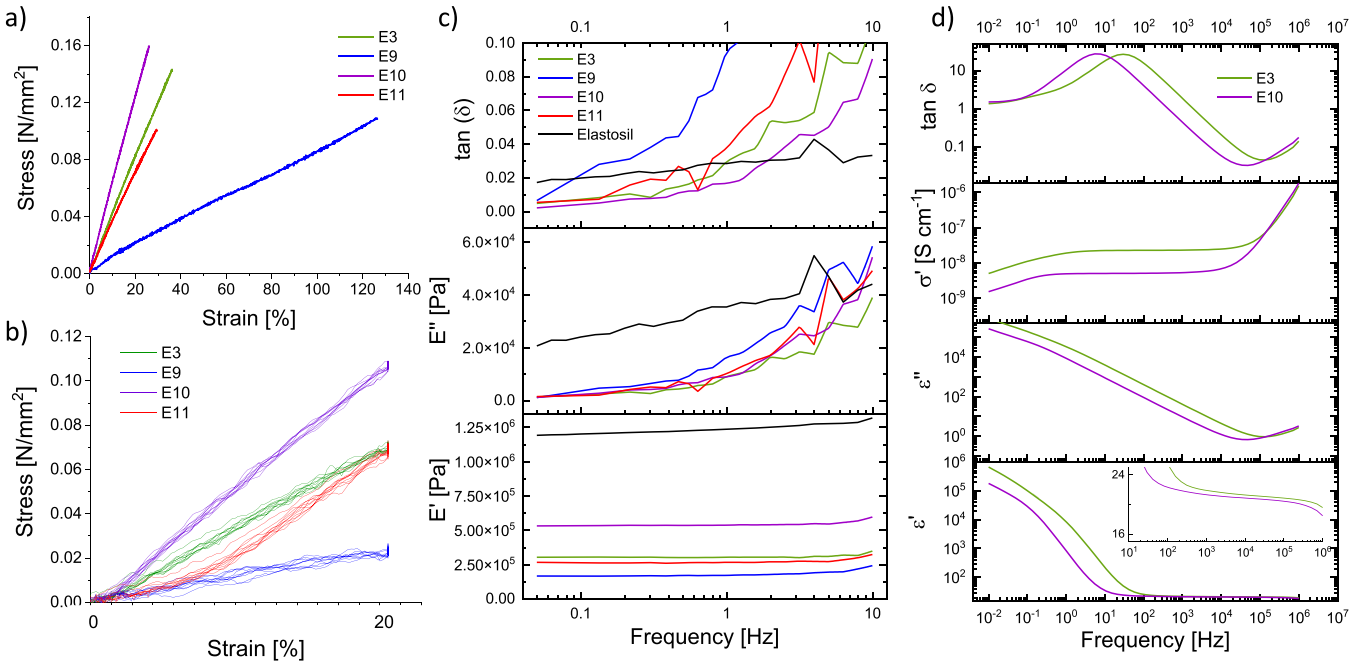

Figure 1. Average stress−strain curves (a). Cyclic uniaxial tensile tests from 0% to 20% strain (b). DMA curves are the average of three different measurements (c) of elastomers **E3**, **E9**, **E10**, and **E11**. Dielectric properties (permittivity (ε'), dielectric loss (ε''), conductivity (σ'), and tan δ) as a function of frequency (d) of elastomers **E3** and **E10**.

and some of their key mechanical properties are summarized in Table 1.

2.2. Mechanical, Thermal, and Dielectric Properties. Stress−strain curves of the different elastomers (Figures S2 and S3, Table 1) revealed that the Young's modulus (Y) at 10% strain of elastomers **E1**−**E9** cross-linked with **CL2**, initially increased from 111 kPa for **E1** to 454 kPa for **E4** with increasing the cross-linker content. However, a further increase in **CL2** resulted in decreasing Y for **E5**−**E9**. In contrast to Y, the average strain at break (s_{av}) initially decreased with increasing **CL2** content from 81% for **E1** to 31% for **E4** and then increased again to reach 153% for **E9** (Figure 1a). These results originate from a change in how the cross-linking agent was incorporated into the network as the ratio of mercapto to vinyl groups becomes larger than one in **E4**−**E9**. **CL2** can cross-link the elastomers either by reacting with two vinyl groups connecting two polysiloxane chains by two thioether groups or by forming a disulfide bridge between two **CL2** moieties. At high **CL2** content, however, it may remain as a side group bound to only one polysiloxane chain and thus function as a plasticizer, decreasing the network's elastic modulus. IR investigations on the cross-linked materials proved to be not sensitive enough to detect the formation of disulfide and thioether groups (Figure S4). When the amount of thiol used was low, the materials were not properly cross-linked, as in the case of **E1**. When the ratio of thiol to vinyl groups was almost 1, as was the case for **E3**, the materials showed good elasticity, but the strain at break was low. When the amount of thiol used was further increased, the strain at break increased as well; however, as will be shown later, the mechanical losses also increased, likely due to dangling chains. Materials **E10** and **E11**, prepared with the same thiol to vinyl ratio as **E3** and **E9** but with **CL4**, exhibited an elastic modulus values of Y = 632 and 363 kPa, respectively. The elastic modulus of material **E10** was thus almost 50% higher than the one of **E3**.

Four materials were then selected for subsequent investigations: two materials cross-linked by **CL2** (**E9** and **E3**) and the two corresponding materials cross-linked by **CL4** (**E10** and **E11**). **E9** was selected because it had the larger strain at break and was among the softest. **E3** and **E4**, in contrast, were among the stiffest in this series, whereby **E3** showed a slightly higher strain at break than **E4**. For the second series of materials, the analogs of **E3** and **E9** were prepared by replacing the difunctional thiol with a tetrafunctional one, while keeping the molar ratio of thiol in **CL4** to the vinyl group in **P** constant. The selected samples were subjected to cyclic uniaxial tensile tests (Figures 1b and S5). Each sample was strained 5 times from 0 to 20% strain and then allowed to relax back to 0% strain. Then, further cyclic tests were conducted by increasing the strain by 20% until the materials ruptured. A minimal hysteresis was observed for all materials, which indicates their good elastic properties (Figure S5).

The tensile testing results suggested that material **E9** might be the most promising candidate for DEAs due to its low Young's modulus, high strain at break, and low mechanical hysteresis. However, actuators constructed with this material showed a drift in the baseline of the actuation strain (Figure S6). Such behavior is typical for elastomers with viscoelastic losses and has been reported before.[31] After being subjected to 1000 actuation cycles at 200−600 V (5.7−17.1 V μm^{-1}), an actuator constructed from **E9** showed some mechanical degradation, such as creep and drift of the baseline, visible at the edge between the active and passive surface (Figure S6 and S7). This is likely due to mechanical losses in the material, which prevent the actuator's full return to the initial state after repetitive actuation. As will be seen later, such degradation is absent in actuators constructed with stiffer materials.

Dynamic mechanical analysis (DMA) was performed to give a better insight into the elastic properties of **E3** and **E9**−**E11** (Figure 1c), in comparison to a commercial PDMS elastomer (Elastosil Film 2030 250) as a reference. The storage modulus

https://doi.org/10.1021/acsami.2c05631
ACS Appl. Mater. Interfaces 2022, 14, 40257−40265

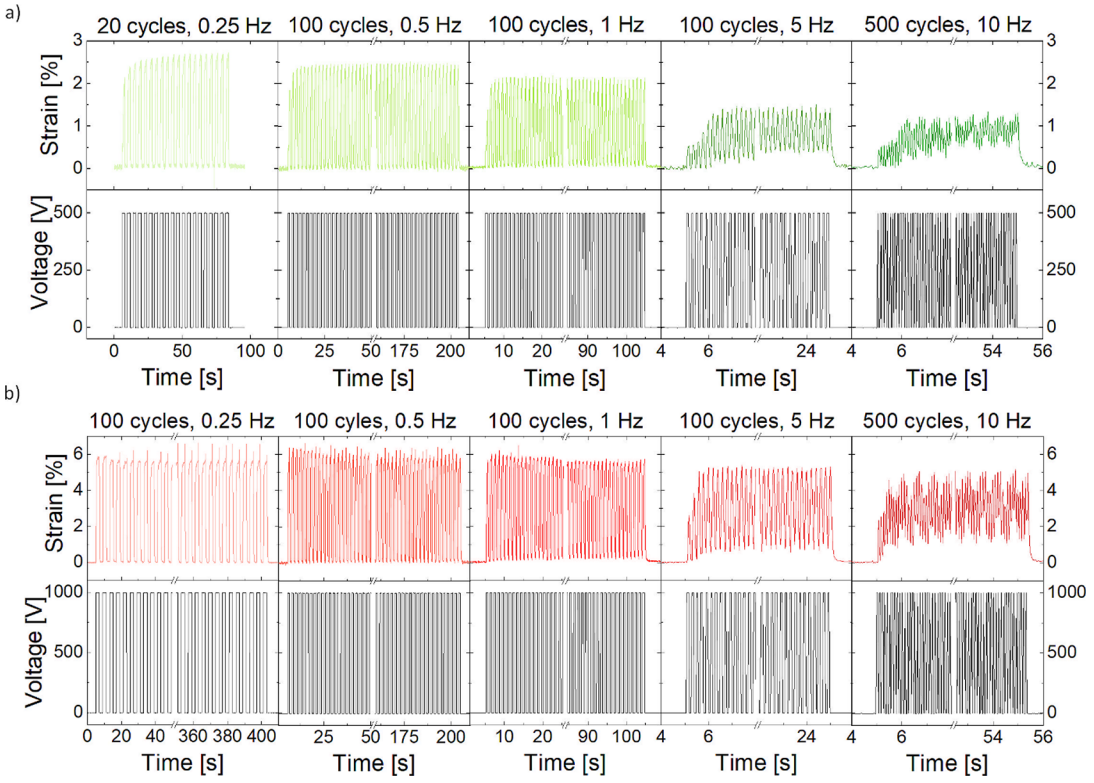

Figure 2. Electromechanical response of an actuator made of material **E3** (122 μm thick) at different frequencies (0.25, 0.5, 1, 5, and 10 Hz): (a) at 500 V; (b) at 1000 V.

values at low frequencies were in good agreement with the Young's modulus Y obtained by tensile testing (Table 1).

The storage modulus is connected to the cross-linking density via:

$$E'(T) = \frac{3\rho RT}{M_{x,\mathrm{eff}}}$$

where $M_{x,\mathrm{eff}}$ is the molar mass of the polymer chain segments between the cross-links.

Material **E10** had a higher storage modulus than **E3**, so its cross-linking density is higher. Although the same molar content of thiol to vinyl groups was used (see Table 1) for the synthesis of materials **E10** and **E3**, E' of **E10** was higher than that of **E3**. The increase in E' of **E10** was hence attributed to the tetrafunctional thiol used, which was assumed to give closer cross-links and make the material stiffer.

All functionalized polymers exhibited a loss factor tan δ below 0.01 at 0.05 Hz, which was even lower than that of Elastosil. At higher frequencies, however, the tan δ of **E3**, **E10**, and **E11** increased to 0.02 at 1−2 Hz, while the tan δ of **E9** showed a sharp increase to 0.1 at 1 Hz. We, therefore, chose materials **E3** and **E10** with the overall lowest tan δ values over the entire frequency range for the subsequent electromechanical tests.

DSC measurements showed that these elastomers had a T_g well-below room temperature (RT), of −41 °C for materials **E3** and **E9** and −37 °C for materials **E10** and **E11** (Figure S8). Since the materials had the same amount of polar groups incorporated and somewhat different elastic moduli, the small T_g difference appeared to be caused by the different thiols used for cross-linking. Because the T_g of these materials is significantly below RT, this small difference in T_g was not expected to impact their RT actuation performance.

The dielectric properties of materials **E3** and **E10** were investigated at different temperatures ranging from −100 to +100 °C (Figure S9). Below T_g, both materials showed a low dielectric permittivity of about 4.5 because the dipoles are frozen and cannot orient in an electric field. Above T_g, the dipoles become mobile and can be polarized, which was reflected by an increase in permittivity to values up to 21 at 10 kHz and 20 °C (Figure 1d). At a frequency of 10^6 Hz, a small decrease in permittivity was observed, which suggested that the dipoles relaxed above this frequency. At frequencies below 10^2 Hz, an apparent increase in the permittivity was observed, which we assigned to the presence of ionic contaminants. These were assumed to come from the starting materials, glassware, or substrate, or have been generated due to contact electrification when removing the films from the substrate. The relaxation frequency for this process was shifted to a lower frequency for material **E10**, which has a higher cross-linking density. The conductivity of both materials at RT remained at 1.2−5 × 10^{-9} S cm^{-1}, and thus was within the range of typical dielectric materials.

2.3. Actuators. A suitable dielectric elastomer for actuator applications should have an increased dielectric permittivity, a high dielectric breakdown field, and an elastic modulus below 1 MPa. Additionally, the dielectric and mechanical losses should be low because they would impact the energy consumption and lifetime of an actuator, which is heated due to these losses. However, we observed that single-membrane actuators gave reliable actuation despite the increased dielectric losses. This is likely due to the easy heat transfer to the environment in single-membrane actuators. The strain at break will not affect the actuation, as it is much larger

https://doi.org/10.1021/acsami.2c05631
ACS Appl. Mater. Interfaces 2022, 14, 40257−40265

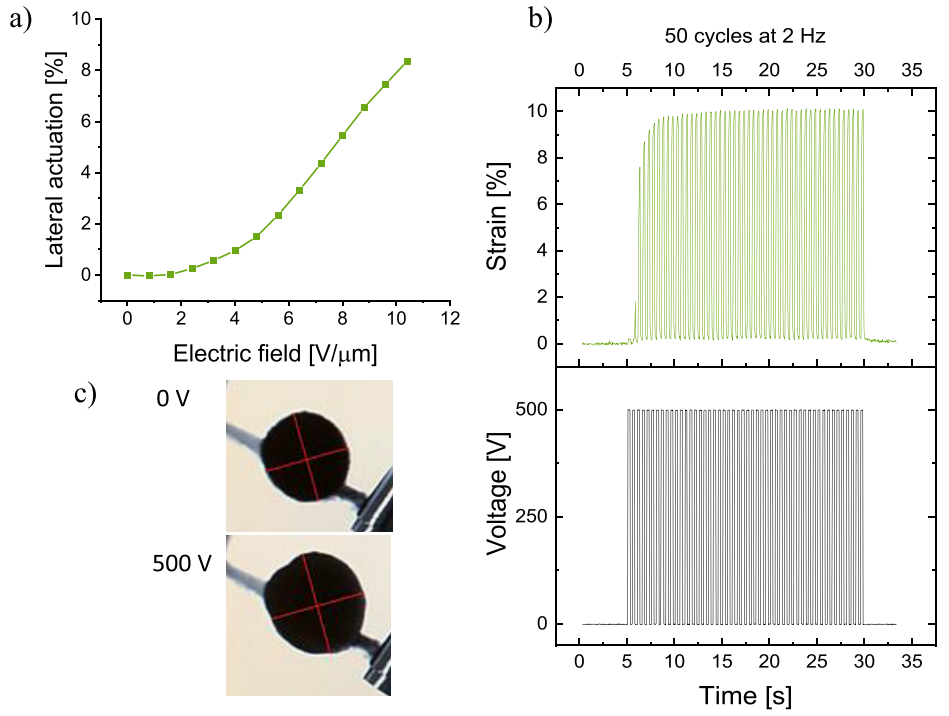

Figure 3. Lateral actuation strain of a 120 μm thick actuator at different electric fields up to the dielectric breakdown of 10.4 V μm^{-1} (a). Lateral actuation strain at 500 V and 2 Hz for 50 cycles (b) of a 66 μm thick actuator made of material **E3**, and photos of the actuator in the relaxed (c, bottom) and actuated (c, top) state at 500 V (7.6 V μm^{-1}).

than the achievable actuation. However, a crucial parameter in actuator performance is the mechanical loss, tan δ, which should be as low as possible to allow for a fast and reversible response. Because of the low mechanical losses of materials **E3** and **E10**, they were further used to construct circular actuators with carbon black electrodes with a diameter of 8 mm. Figure 2 shows the actuation at different frequencies for a film of **E3** (thickness 122 μm) at actuation voltages of 500 and 1000 V, respectively. At 500 V (4.1 V μm^{-1}), the actuation showed a more pronounced frequency dependence than that at 1000 V (8.2 V μm^{-1}). For instance, at 0.25 Hz and 500 V, the actuator exhibited a 2.7% lateral actuation strain, while at 10 Hz, the actuation decreased by half. When the voltage was increased to 1000 V, the lateral actuation strain increased to 6% at 0.25 Hz and was reduced to 5% by increasing the frequency to 10 Hz. Actuators made from **E3** and **E9** actuated for more than 1000 cycles and showed no visible degradation for **E3** but some degradation for **E9** (Figure S7).

A second actuator made of **E3** (thickness 120 μm) gave 5% strain at 0.25 Hz and 750 V, corresponding to 6.25 V μm^{-1} (Figure S10). It survived 30 000 cycles at 5 Hz, showing 4% lateral actuation strain at 750 V. When the voltage was increased from 0 V to the breakdown voltage in steps of 100 V, the actuator showed a maximum lateral actuation of 8.3% at 10.4 V μm^{-1} where the it suffered a breakdown (Figure 3a).

The third actuator of **E3** (thickness 138 μm) gave 1−2% lateral actuation at low electric fields (2.9−3.6 V μm^{-1}) and survived more than 450 000 actuation cycles (Figure S11). However, the actuation strain was reduced during the last 150 000 cycles. After this, the voltage was increased to reach the breakdown, which occurred at 6.5 V μm^{-1}. The large number of electromechanical cycles clearly show the potential of this material for actuator applications.

The best actuator made of **E3** (thickness 66 μm) gave the highest lateral actuation of almost 10% at 2 Hz and 500 V (Figure 3, Video S1), corresponding to 7.6 V μm^{-1}. When the material was tested for 20 000 cycles at 500 V and 5 Hz, a decrease in lateral actuation from 10 to 6.5% was observed (Figure S12). This decrease may be due to dielectric or electrode degradation and has been observed before in other dielectric materials.[32]

Material **E10** showed inferior actuation compared to **E3**, supposedly due to its higher elastic modulus (Figures S13 and S14). More information regarding the actuation of **E10** can be found in the Supporting Information.

The breakdown strength of materials **E3** and **E10** was tested by placing films between two metallic electrodes with a 1 mm^2 active area. The voltage was gradually increased until the breakdown occurred. Ten samples for each elastomer were tested. Materials **E3** and **E10** showed a breakdown field strengths, E_b, of 18.2 ± 2.0 V and 26.6 ± 4.3 V μm^{-1}, respectively. The measured values are in good agreement with those predicted for homogeneous elastomers according to the formula $E_b = 0.6 \times [Y/(2\varepsilon_0\varepsilon_r)]^{0.5}$ derived by Stark and Garton,[33,34] of 20.4 V μm^{-1} for **E3** and 24.7 V μm^{-1} for **E10**. The dielectric breakdown field strength decrease is characteristic of soft elastomers with increased dielectric permittivity.

2.4. Sensors. High dielectric permittivity elastomers are attractive not only as dielectrics in actuators but also in stretchable capacitive sensors. Such sensors may find applications in personalized medicine, where degradable high dielectric permittivity elastomers may be advantageous. For this application, the elastic modulus should be low to allow easy deformation by small forces, the strain at break should be sufficiently high to stress the materials at different strain levels, and the dielectric permittivity should be high to increase sensor sensitivity. The dielectric losses will practically not

https://doi.org/10.1021/acsami.2c05631
ACS Appl. Mater. Interfaces 2022, 14, 40257−40265

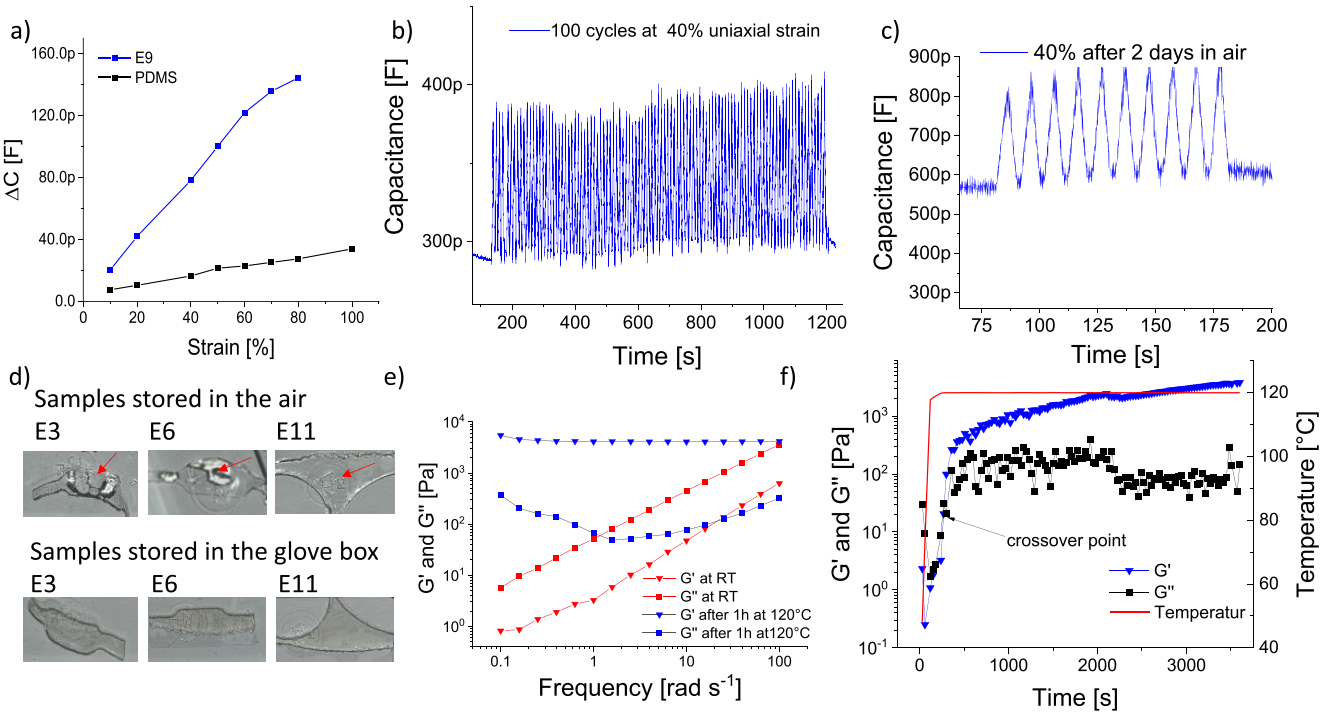

Figure 4. Change in capacitance with strain for **E9** and PDMS (a). Change in capacitance over 100 cycles at 40% strain for a sensor from **E9** stored in a vacuum oven (b) and after storing for 2 days in air (c). Photo of samples **E3**, **E6**, and **E11** stored in the air (d, top) and in a glovebox (d, bottom); rheological measurements of depolymerized sample **ES3** before and after cross-linking at elevated temperature (e). Time-dependent rheological measurement at 120 °C and 1 rad s^{-1} every 30 s (f).

impact sensor performance as the applied operation voltage is very low (about 1 V).

Material **E9** was selected because of its high strain at break of 153% and low Young's modulus of 112 kPa. This material was compared with PDMS films, the currently most explored dielectric in capacitive sensors. The slope of the change in capacitance as a function of the applied strain as a measure of the sensor sensitivity[35] increased from 0.29 pF for PDMS to 1.84 pF for **E9** (Figure 4a), representing an increase in sensitivity of more than 6 times. The change in capacitance for **E9** at 40% strain during 100 cycles is presented in Figure 4b. The sensor showed a reversible change in capacitance from 290 pF at 0% strain to 380 pF at 40% strain over 100 stretching cycles, respectively. The change in capacitance was reversible even for sensors strained by 80% for over 10 cycles (Figure S15).

We observed that the capacitance of the sensor changed when stored for 2 days in the air. An almost 2-fold increase in the initial capacitance from 290 pF for the dried sensor to 590 pF for the one stored in the air was observed (Figure 4b,c). Thus, ΔC at 40% strain increased from 90 pF for the dried sensor to 290 pF for the sensor kept in the air. This is an indication that the material is susceptible to water uptake from the environment, which may require encapsulation for practical applications. Water diffusion can, for instance, be controlled with organic transient encapsulates, which extend the lifetime of transient devices to desired periods.[4] Moreover, this change of capacitance due to water uptake may be attractive for monitoring water in dry environments (e.g., glove boxes), sensing damages of installations or equipment, or anywhere where water is undesirable, and thus, such capacitive sensors may detect a leakage preventing catastrophic damages.

2.5. Re-Cross-Linking. During our investigations, we observed that when samples **E3**, **E6**, and **E11** were stored in air, they slowly disintegrated over a period of 180 days, while they remained stable over the same duration when stored in a glovebox (Figure 4d). The different elastomers disintegrated to different extents. For instance, material **E11** disintegrated more slowly than **E3** and **E6**. While the latter elastomers changed to liquid droplets, sample **E11** kept its shape but turned more viscoelastic. We attributed the slower disintegration of **E11** to the higher degree of cross-linking and a decreased mobility of the chains. The disintegration is rather slow, taking months for a visible change. We suspect that ambient moisture causes the disintegration by depolymerizing the polysiloxane backbone and forming shorter polysiloxane chains with silanol end groups. Dynamic vapor sorption (DVS) experiments clearly showed the affinity of our materials to absorb water (Figure S16), due to their increased polarity. It should be mentioned that no such cleavage was observed before for polar polysiloxanes modified with nitrile, nitroaniline, thioether, or sulphonyl groups at RT for which the same synthesis strategy was used. While the uptake of water is rather fast, the depolymerization process took months nevertheless, likely due to the low concentration of active silanolates and the low mobility of the chain ends since the materials are chemically cross-linked.

^{1}H NMR of starting polymer **P** and material **E3** after depolymerization show no degradation of the amide side groups (Figure S17). Aliphatic primary, secondary, and tertiary amines are known to undergo nucleophilic cleavage of Si−O bonds.[30] Thus, polysiloxanes are known to be sensitive to humidity under basic and acidic conditions and to undergo depolymerization. Depolymerization occurs, for example, in the presence of metal hydroxides such as KOH and requires

https://doi.org/10.1021/acsami.2c05631
ACS Appl. Mater. Interfaces 2022, 14, 40257−40265

elevated temperatures. This is due to the reported strong interaction between the potassium cation and the silanolate anion, which reduces the nucleophilicity of the silanolate and consequently lowers the rate of depolymerization. The nucleophilicity of the silanolate anion is significantly increased if the coordination with the counterion is weak. Such "naked" anions have higher reactivity than sodium and potassium hydroxide. A recent investigation showed that silanolates in a "naked" form, due to their low complexation with the counterion, undergo fast solvent-free depolymerization of polydimethylsiloxanes.[36] The polysiloxane used for synthesizing our materials has silanol end groups, which can, in principle, be deprotonated to silanolates either by traces of bases or by forming hydrogen-bridge networks with the oxygen or nitrogen atoms of the amides in the side chains. The formed silanolate will then undergo depolymerization by the silanolate nucleophilically attacking a silicon in the main chain. Thus, during depolymerization, the Si−O−Si bonds are cleaved with the formation of Si−OH groups.

The IR spectrum of the depolymerized sample showed signals of the silanol groups characterized by their OH absorption bands at 3800−3000 cm^{-1} as well as an Si−O stretch near 940 cm^{-1} (Figure S18). After the polymer was heated to 120 °C, the materials was re-crosslinked, as indicated by rheological measurements (Figure 4f). The silanol end groups condense with formation of Si−O−Si bonds and water, and the characteristic signals for the silanol groups were significantly reduced (Figure S18).

Additionally, a depolymerized sample was heated to 120 °C in a TGA, and the released compounds were analyzed by a mass spectrometer (Figure S19). The MS allowed us to prove that, indeed, water was released during heating. This water is due to the adsorption and condensation of the silanol groups to Si−O−Si, as confirmed by the disappearance of the Si−O stretch near 940 cm^{-1} (Figure S18).

To investigate the possibility of re-cross-linking, depolymerized material **E3** was heated to 120 °C, where two silanol groups condensed with the formation of a Si−O−Si bond and water, which evaporated. The heated material solidified within 20 min. Rheological measurements conducted on a depolymerized sample and a heat-treated one support this. The depolymerized sample shows a typical liquid behavior at RT, with a storage modulus G' below the loss modulus G'' over the entire frequency range (Figure 4e, red curve). The time-dependent rheological measurement at 120 °C and 1 rad s^{-1} shows a crossover of G' and G'' after 280 s, which indicates that the material solidified (Figure 4f). After keeping the material for 60 min at 120 °C, another frequency-dependent measurement at RT was conducted (Figure 4e, blue curve) and showed that G' was significantly higher than G''.

3. CONCLUSION

Novel elastomers with an increased dielectric permittivity of 21 based on polysiloxane modified with polar *N,N*-dimethyl-3-thiopropanamide side groups were synthesized via a thiol−ene postpolymerization modification of polymethylvinylsiloxane with less than stoichiometric amount of *N,N*-dimethyl-3-mercaptopropanamide to vinyl groups followed by thiol−ene cross-linking with multifunctional thiols. Elastomers with Young's modulus in the range from 111 to 632 kPa, and strain at break from 28 to 153% were synthesized. The elastomers exhibit low glass transition temperatures (−37 °C and −41 °C) and low viscous losses below the value of a commercial polydimethylsiloxane elastomer at low frequencies. Some actuators withstood 450,000 actuation cycles at electric fields below 3.6 V μm^{-1} and gave an actuation strain in the range of 1.2−1.8%. The best actuator showed almost 10% strain at only 7.6 V μm^{-1} (500 V), which reflects the potential of our material for low voltage applications (Video S1). Capacitive sensors exhibited a 6-fold increase in sensitivity for the polar elastomer compared to conventional silicone rubber. Depolymerization of these materials under ambient conditions opens the possibility of using them in transient electronics and the possibility of recycling.

4. EXPERIMENTAL SECTION/METHODS

4.1. Materials. Unless otherwise stated, all chemicals were reagent grade and used without purification. 1,3,5,7-Tetramethyl-1,3,5,7-tetravinyl cyclotetrasiloxane (V_4) was purchased from ABCR. 2,2-Dimethoxy-2-phenylacetophenone (DMPA), 2,2′-(ethylenedioxy)-diethanethiol, benzene, toluene, sodium hydroxide, *N,N*-dimethylacrylamide, tetramethylammonium hydroxide 25% in methanol (TMAH), hydrochloric acid, and thioacetic acid were purchased from Aldrich. Methanol and tetrahydrofuran were purchased from VWR. As a sacrificial layer, we used a solution of PVA in isopropanol/2-butanol from Suter Kunststoffe AG. Elastosil Film 2030 250 with a thickness of 200 μm and cross-linkable electrode Elastosil LR 3162A/B were purchased from Wacker. Polymethylvinylsiloxane (**PV**) (M_n = 105 480 g mol^{-1}, M_w = 375 000 g mol^{-1}, PDI = 3.55) and *N,N*-dimethyl-3-mercaptopropanamide were prepared according to the literature.[12]

4.2. Characterization. The description of the setup used for the characterization of polymers and elastomers was described elsewhere and can be found in the Supporting Information.[32]

For fabrication of the sensor, one layer of elastomer (PDMS or **E*x***) was covered with cross-linked electrodes Elastosil LR 3162A/B on both sides. The electrode was prepared as follows. First, defined amounts of the two components were weighted into a vial and the same weight of toluene was added and the resulting mixture mechanically mixed with a spatula. The two mixtures were let stand at RT for 1 day. Thereafter, they were diluted to reach a ratio of composite/toluene = 1:4. The addition was done portion-wise to ensure good mixing. After all the solvent was added, the two components were separately mixed using an ultraspeed mixer until they turned homogeneous. Thereafter, a 1:1 mixture of the two components was mechanically mixed and blade-coated on a Teflon substrate, where the solvent was allowed to evaporate at RT for 30 min. Thereafter the films were cross-linked at 120 °C for 1 h. The cross-linked film was additionally dried for 12 h in a vacuum oven at 60 °C. Thickness of the obtained film was around 20 μm. From the obtained film, stripes with a width of 10 mm were cut.

The active sensing area had the following dimensions: 25 × 10 × 0.2 mm. To insulate the sensor, VHB 4910 film from 3M was used. It was cut into strips with a width of 2 cm, and the sensors were sandwiched between two such stripes. Each sensor was cycled 10 times at 10, 20, 40, 50, 60, 70, and 80% strain. From each measurement, the average capacitance in strained form was taken. From this value, the average capacitance in unstrained form was subtracted, and the graph ΔC versus applied strain was obtained.

4.3. General Synthesis of Polysiloxane Containing *N,N*-Dimethyl-3-mercaptopropanamide and 3.3% Vinyl Groups (P). **PV** (10 g, 0.116 mol repeat units, 1 equiv), *N,N*-dimethyl-3-mercaptopropanamide (14.7 g, 0.11 mol, 0.95 equiv), and DMPA (0.297 g, 1.16 mmol, 0.01 equiv) were dissolved in 250 mL of THF. The reaction mixture was degassed three times using the freeze−pump−thaw technique and irradiated for 20 min with UV light. The solution was concentrated with a rotary evaporator, and the polymer was purified three times by dissolving it in THF and precipitating it in cyclohexane. The obtained polymer was dissolved in THF, filtered through a glass filter, and the solvent was evaporated. Finally, the concentration of polymer was adjusted to 70 wt % in THF. ^{1}H NMR

https://doi.org/10.1021/acsami.2c05631
ACS Appl. Mater. Interfaces 2022, 14, 40257−40265

($CDCl_3$, 400 MHz), δ: 2.97 (s, 3H), 2.92 (s, 3H), 2.77 (q, 2H), 2.62 (t, 2H), 1.74 (t, 1H). ^{13}C NMR ($CDCl_3$, 100 MHz), δ: 170.8; 37.3; 37.1; 35.4; 20.1.

Formation of Polar Elastomers (Ex). Polymer **P** (1.43 g of 70 wt % **P** in THF) was mixed with a certain amount of cross-linker (for amounts, see Table 1) and DMPA (4.5 mg). The obtained mixture was centrifuged for 2 min at 6000 rpm to remove the bubbles. Thick films (>80 μm) were cast directly on a Teflon substrate, while thin films were cast on a glass coated with a sacrificial PVA layer. Thick films were kept in air for 30 min to allow the solvent to evaporate, then cross-linked by irradiation with UV light for 5 min at a distance of 15 cm from the substrate. During our previous work, we observed that high internal stress was created if polar polysiloxane was cast from a solution with high solvent content and directly irradiated with UV light. The cross-linked film either showed extreme bending when detached from the substrate, or it ruptured on the substrate. For cross-linking, a mercury vapor UV-light source UVAHAND 250 GSH1 from Dr. Hönle AG without additional filters provided an irradiation intensity of 15 mW cm^{-2} in the frequency range between 320 and 600 nm. Thereafter, the films were dried for 12 h in the vacuum oven at 60 °C. Thin films were cross-linked directly after casting, and after dissolving the PVA layer, they were dried in the vacuum oven at 60 °C. Before all tests, materials were stored in the vacuum oven at 60 °C.

■ ASSOCIATED CONTENT

Supporting Information

The Supporting Information is available free of charge at https://pubs.acs.org/doi/10.1021/acsami.2c05631.

GPC data of the starting polymers, ^1H NMR spectra, IR of the cross-linked films, tensile test, cyclic tensile test, DSC, broadband impedance spectroscopy data from −100 to +100 °C, capacitance change with strain, DVS curves, TGA/MS of the depolymerized network, cyclic electromechanical tests of **E3** and **E10** (PDF)

Video showing cyclic electromechanical test of **E3** (MP4)

■ AUTHOR INFORMATION

Corresponding Author

Dorina M. Opris − *Functional Polymers, Empa, Swiss Federal Laboratories for Materials Science and Technology, 8600 Dübendorf, Switzerlandh;* orcid.org/0000-0002-0585-7500; Email: dorina.opris@empa.ch

Authors

Yauhen Sheima − *Functional Polymers, Empa, Swiss Federal Laboratories for Materials Science and Technology, 8600 Dübendorf, Switzerlandh; Ecole Polytechnique Fédérale de Lausanne (EPFL), Institut des Matériaux, CH 1015 Lausanne, Switzerland*

Johannes von Szczepanski − *Functional Polymers, Empa, Swiss Federal Laboratories for Materials Science and Technology, 8600 Dübendorf, Switzerlandh*

Patrick M. Danner − *Functional Polymers, Empa, Swiss Federal Laboratories for Materials Science and Technology, 8600 Dübendorf, Switzerlandh*

Tina Künniger − *Laboratory for Cellulose and Wood Materials, Empa, Swiss Federal Laboratories for Materials Science and Technology, 8600 Dübendorf, Switzerland*

Arndt Remhof − *Materials for Energy Conversion, Empa, Swiss Federal Laboratories for Materials Science and Technology, 8600 Dübendorf, Switzerland;* orcid.org/0000-0002-8394-9646

Holger Frauenrath − *Ecole Polytechnique Fédérale de Lausanne (EPFL), Institut des Matériaux, CH 1015 Lausanne, Switzerland;* orcid.org/0000-0002-1720-6991

Complete contact information is available at: https://pubs.acs.org/10.1021/acsami.2c05631

Notes

The authors declare no competing financial interest.

■ ACKNOWLEDGMENTS

We gratefully acknowledge the Swiss National Science Foundation (200020_172693 and 206021_150638/1), the EU Marie Curie ITN project SMART (860108), the European Research Council (ERC) under the European Union's Horizon 2020 research and innovation programme (grant agreement No 101001182), and the ETH Board for the project MANUFHAPTICS in the framework of the Strategic Focus Area (SFA) Advanced Manufacturing and the Swiss Federal Laboratories for Materials Science and Technology (Empa, Dübendorf) for financial support. We also acknowledge B. Fischer (Empa) for GPC, DSC, and TGA measurements, Dr. G. Kovacs (Empa) for providing access to the electromechanical test equipment, L. Düring (CT Systems) for his continuous support with technical issues, and Dr. D. Rentsch (Empa) for his support with the NMR measurements. D.M.O. thanks Prof. F. A. Nüesch (Empa) for the freedom to perform this research and his continuous support.

■ ABBREVIATIONS

DEs, dielectric elastomers; **PV**, polymethylvinylsiloxane; **CL**, cross-linker; **CL2**, 2,2′-(ethylenedioxy)diethanethiol; **CL4**, pentaerythritol tetrakis(3-mercaptopropionate); **E**, elastomer; PDMS, polydimethylsiloxane

■ REFERENCES

(1) Tiseo, I. Electronic waste generated worldwide from 2010 to 2019 (in million metric tons). *Global e-waste generation 2010-2019, Statista*, March 2021. https://www.statista.com/statistics/499891/projection-ewaste-generation-worldwide (accessed 2022−03−30).

(2) Sthiannopkao, S.; Wong, M. H. Handling E-Waste in Developed and Developing Countries: Initiatives, Practices, and Consequences. *Sci. Total Environ.* **2013**, *463−464*, 1147−1153.

(3) Cheng, H.; Vepachedu, V. Recent Development of Transient Electronics. *Theor. Appl. Mech. Lett.* **2016**, *6*, 21−31.

(4) Shim, J. S.; Rogers, J. A.; Kang, S. K. Physically Transient Electronic Materials and Devices. *Mater. Sci. Eng. R Reports* **2021**, *145*, 100624.

(5) Morganti, P.; Coltelli, M.-B. A New Carrier for Advanced Cosmeceuticals. *Cosmetics* **2019**, *6*, 10.

(6) Wu, G.; Zhang, J.; Wan, X.; Yang, Y.; Jiang, S. Chitosan-Based Biopolysaccharide Proton Conductors for Synaptic Transistors on Paper Substrates. *J. Mater. Chem. C* **2014**, *2*, 6249−6255.

(7) Liu, Y. H.; Zhu, L. Q.; Feng, P.; Shi, Y.; Wan, Q. Freestanding Artificial Synapses Based on Laterally Proton-Coupled Transistors on Chitosan Membranes. *Adv. Mater.* **2015**, *27*, 5599−5604.

(8) Durukan, M. B.; Cicek, M. O.; Doganay, D.; Gorur, M. C.; Çınar, S.; Unalan, H. E. Multifunctional and Physically Transient Supercapacitors, Triboelectric Nanogenerators, and Capacitive Sensors. *Adv. Funct. Mater.* **2022**, *32*, 2106066.

(9) Parashkov, R.; Becker, E.; Hartmann, S.; Ginev, G.; Schneider, D.; Krautwald, H.; Dobbertin, T.; Metzdorf, D.; Brunetti, F.; Schildknecht, C.; Kammoun, A.; Brandes, M.; Riedl, T.; Johannes, H.-H.; Kowalsky, W. Vertical Channel All-Organic Thin-Film Transistors. *Appl. Phys. Lett.* **2003**, *82*, 4579.

(10) Opris, D. M. Polar Elastomers as Novel Materials for Electromechanical Actuator Applications. *Adv. Mater.* **2018**, *30*, 1703678.
(11) Hwang, S. W.; Park, G.; Cheng, H.; Song, J. K.; Kang, S. K.; Yin, L.; Kim, J. H.; Omenetto, F. G.; Huang, Y.; Lee, K. M.; Rogers, J. A. 25th Anniversary Article: Materials for High-Performance Biodegradable Semiconductor Devices. *Adv. Mater.* **2014**, *26*, 1992−2000.
(12) Sheima, Y.; Yuts, Y.; Frauenrath, H.; Opris, D. M. Polysiloxanes Modified with Different Types and Contents of Polar Groups: Synthesis, Structure, and Thermal and Dielectric Properties. *Macromolecules* **2021**, *54*, 5737−5749.
(13) Ning, N.; Qin, H.; Wang, M.; Sun, H.; Tian, M.; Zhang, L. Improved Dielectric and Actuated Performance of Thermoplastic Polyurethane by Blending with XNBR as Macromolecular Dielectrics. *Polymer* **2019**, *179*, 121646.
(14) Sheima, Y.; Caspari, P.; Opris, D. M. Artificial Muscles: Dielectric Elastomers Responsive to Low Voltages. *Macromol. Rapid Commun.* **2019**, *40*, 1900205.
(15) Madsen, F. B.; Yu, L.; Daugaard, A. E.; Hvilsted, S.; Skov, A. L. Silicone Elastomers with High Dielectric Permittivity and High Dielectric Breakdown Strength Based on Dipolar Copolymers. *Polymer.* **2014**, *55*, 6212−6219.
(16) Racles, C.; Cazacu, M.; Fischer, B.; Opris, D. M. Synthesis and Characterization of Silicones Containing Cyanopropyl Groups and Their Use in Dielectric Elastomer Actuators. *Smart Mater. Struct.* **2013**, *22*, 104004.
(17) Turcan-Trofin, G. O.; Asandulesa, M.; Balan-Porcarasu, M.; Varganici, C. D.; Tiron, V.; Racles, C.; Cazacu, M. Linear and Cyclic Siloxanes Functionalized with Polar Groups by Thiol-Ene Addition: Synthesis, Characterization and Exploring Some Material Behaviour. *J. Mol. Liq.* **2019**, *282*, 187−196.
(18) Kussmaul, B.; Risse, S.; Kofod, G.; Waché, R.; Wegener, M.; McCarthy, D. N.; Krüger, H.; Gerhard, R. Enhancement of Dielectric Permittivity and Electromechanical Response in Silicone Elastomers: Molecular Grafting of Organic Dipoles to the Macromolecular Network. *Adv. Funct. Mater.* **2011**, *21*, 4589−4594.
(19) Hu, W.; Zhang, S. N.; Niu, X.; Liu, C.; Pei, Q. An Aluminum Nanoparticle-Acrylate Copolymer Nanocomposite as a Dielectric Elastomer with a High Dielectric Constant. *J. Mater. Chem. C* **2014**, *2*, 1658−1666.
(20) Li, C. H.; Wang, C.; Keplinger, C.; Zuo, J. L.; Jin, L.; Sun, Y.; Zheng, P.; Cao, Y.; Lissel, F.; Linder, C.; You, X. Z.; Bao, Z. A Highly Stretchable Autonomous Self-Healing Elastomer. *Nat. Chem.* **2016**, *8*, 618−624.
(21) Zhang, Q.; Niu, S.; Wang, L.; Lopez, J.; Chen, S.; Cai, Y.; Du, R.; Liu, Y.; Lai, J. C.; Liu, L.; Li, C. H.; Yan, X.; Liu, C.; Tok, J. B. H.; Jia, X.; Bao, Z. An Elastic Autonomous Self-Healing Capacitive Sensor Based on a Dynamic Dual Crosslinked Chemical System. *Adv. Mater.* **2018**, *30*, 1801435.
(22) Ren, Z.; Hu, W.; Liu, C.; Li, S.; Niu, X.; Pei, Q. Phase-Changing Bistable Electroactive Polymer Exhibiting Sharp Rigid-to-Rubbery Transition. *Macromolecules* **2016**, *49*, 134−140.
(23) Chortos, A.; Hajiesmaili, E.; Morales, J.; Clarke, D. R.; Lewis, J. A. 3D Printing of Interdigitated Dielectric Elastomer Actuators. *Adv. Funct. Mater.* **2020**, *30*, 1907375.
(24) Zhang, L.; Wang, D.; Hu, P.; Zha, J. W.; You, F.; Li, S. T.; Dang, Z. M. Highly Improved Electro-Actuation of Dielectric Elastomers by Molecular Grafting of Azobenzenes to Silicon Rubber. *J. Mater. Chem. C* **2015**, *3*, 4883−4889.
(25) Yang, D.; Ge, F.; Tian, M.; Ning, N.; Zhang, L.; Zhao, C.; Ito, K.; Nishi, T.; Wang, H.; Luan, Y. Dielectric Elastomer Actuator with Excellent Electromechanical Performance Using Slide-Ring Materials/Barium Titanate Composites. *J. Mater. Chem. A* **2015**, *3*, 9468−9479.
(26) Tan, M. W. M.; Thangavel, G.; Lee, P. S. Enhancing Dynamic Actuation Performance of Dielectric Elastomer Actuators by Tuning Viscoelastic Effects with Polar Crosslinking. *NPG Asia Mater.* **2019**, *11*, 62.
(27) Sun, H.; Liu, X.; Yu, B.; Feng, Z.; Ning, N.; Hu, G. H.; Tian, M.; Zhang, L. Simultaneously Improved Dielectric and Mechanical Properties of Silicone Elastomer by Designing a Dual Crosslinking Network. *Polym. Chem.* **2019**, *10*, 633−645.
(28) Sun, H.; Liu, X.; Liu, S.; Yu, B.; Ning, N.; Tian, M.; Zhang, L. Silicone Dielectric Elastomer with Improved Actuated Strain at Low Electric Field and High Self-Healing Efficiency by Constructing Supramolecular Network. *Chem. Eng. J.* **2020**, *384*, 123242.
(29) Yang, D.; Tian, M.; Kang, H.; Dong, Y.; Liu, H.; Yu, Y.; Zhang, L. New Polyester Dielectric Elastomer with Large Actuated Strain at Low Electric Field. *Mater. Lett.* **2012**, *76*, 229−232.
(30) Hsiao, Y. -C; Hill, L. W.; Pappas, S. P. Reversible Amine Solubilization of Cured Siloxane Polymers. *J. Appl. Polym. Sci.* **1975**, *19*, 2817−2820.
(31) Opris, M. D.; Molberg, M.; Nüesch, F.; Löwe, C.; Walder, C.; Fischer, B. Dielectric Elastomer Materials for Actuators and Energy Harvesting. *Proc. SPIE* **2011**, *7976*, 79760G.
(32) Caspari, P.; Nüesch, F. A.; Opris, D. M. Synthesis of Solvent-Free Processable and on-Demand Cross-Linkable Dielectric Elastomers for Actuators. *J. Mater. Chem. C* **2019**, *7*, 12139−12150.
(33) Stark, K. H.; Garton, C. G. Electric Strength of Irradiated Polythene. *Nature* **1955**, *176*, 1225−1226.
(34) Carpi, F.; Gallone, G.; Galantini, F.; De Rossi, D. *Enhancing the Dielectric Permittivity of Elastomers*; Elsevier, 2008.
(35) Kollosche, M.; Stoyanov, H.; Laflamme, S.; Kofod, G. Strongly Enhanced Sensitivity in Elastic Capacitive Strain Sensors. *J. Mater. Chem.* **2011**, *21*, 8292−8294.
(36) Weitkamp, R. F.; Neumann, B.; Stammler, H.-G.; Hoge, B. Synthesis and Reactivity of the First Isolated Hydrogen-Bridged Silanol-Silanolate Anions. *Angew. Chem., Int. Ed.* **2020**, *59*, 5494−5499.

https://doi.org/10.1021/acsami.2c05631
ACS Appl. Mater. Interfaces 2022, 14, 40257−40265